

# Molecular Packing and NPT-Molecular Dynamics Investigation of the Transferability of the RDX Intermolecular Potential to 2,4,6,8,10,12-Hexanitrohexaazaisowurtzitane

Dan C. Sorescu,<sup>†,‡</sup> Betsy M. Rice,<sup>\*,§</sup> and Donald L. Thompson<sup>†</sup>

Department of Chemistry, Oklahoma State University, Stillwater, Oklahoma 74078, and  
The U.S. Army Research Laboratory, Aberdeen Proving Ground, Maryland 21005

Received: October 1, 1997; In Final Form: November 19, 1997

We have explored the degree to which an intermolecular potential for the explosive hexahydro-1,3,5-trinitro-1,3,5-*s*-triazine (RDX) (*J. Phys. Chem. B* **1997** 101, 798) is transferable for predictions of crystal structures (within the approximation of rigid molecules) of a similar chemical system, in this case, polymorphic phases of the 2,4,6,8,10,12-hexanitrohexaazaisowurtzitane (HNIW) crystal. Molecular packing and isothermal–isobaric molecular dynamics calculations performed with this potential reproduce the main crystallographic features of the  $\epsilon$ -,  $\beta$ -, and  $\gamma$ -HNIW crystals. Thermal expansion coefficients calculated using the present model predict near isotropic expansion for the  $\epsilon$ - and  $\gamma$ -HNIW crystal phases and anisotropic expansion for  $\beta$ -HNIW.

## Introduction

Satisfying ever-increasing demands for inexpensive, efficient, and rapid development of high-performing energetic materials is extremely challenging. Synthesis and testing of energetics is often costly, dangerous, and time-consuming; thus, a screening mechanism is needed to reduce unnecessary measurements on unsuitable candidate materials. Such screening can be accomplished through the application of theoretical chemical models. These models can be used to predict simple thermodynamic properties of the candidates, such as heats of formation or the density of the material, which are sufficient to aid formulators in decisions of whether a candidate energetic material warrants further investigation. Due to timely advances in parallel computer architectures, there is great promise that atomistic modeling will become integral to the development process. In addition to being efficient screening tools, theoretical chemical models can also provide atomic-level information that could not otherwise be readily obtained through measurement.

Our efforts at developing accurate predictive models of energetic crystals have included the development of an intermolecular potential that describes the structure of the  $\alpha$ -form of the hexahydro-1,3,5-trinitro-1,3,5-*s*-triazine (RDX) crystal, one of the most commonly used explosives.<sup>1</sup> The potential energy function that describes the system is composed of pairwise atom–atom (6-exp) Buckingham interactions with explicit inclusion of the electrostatic interactions between the charges associated with various atoms of different molecules. The parametrization of the potential function was done such that molecular packing (MP) calculations reproduce the experimental structure of the crystal and its lattice energy. Isothermal–isobaric molecular dynamics simulations (NPT-MD) using this potential energy function predicted crystal structures in excellent agreement with experiment. The main limitation of the model is due to the assumption of rigid molecules. Nevertheless, it

can be used to study processes at temperatures and pressures where molecular deformations are negligible.

The development of a simple model that accurately represents a specific chemical system is significant. However, the utility of the model is substantially enhanced if it reasonably represents a series of chemical systems rather than a single one. This investigation explores the degree of transferability of the RDX crystal potential energy function<sup>1</sup> to another cyclic nitramine crystal, that is, the new explosive, 2,4,6,8,10,12-hexanitrohexaazaisowurtzitane (HNIW) (see Figure 1).

HNIW, a polycyclic nitramine, has been characterized as “the densest and most energetic explosive known.”<sup>2</sup> It exists in at least five polymorphic states,<sup>3</sup> four of which ( $\alpha$ -hydrate,  $\epsilon$ ,  $\beta$ , and  $\gamma$ ) are stable at ambient conditions and have been resolved by X-ray diffraction.<sup>4</sup> The  $\alpha$ -hydrate phase has an orthorhombic structure with *Pbca* symmetry and with *Z* = 8 molecules per unit cell;<sup>5</sup> the  $\epsilon$ -polymorph crystallizes in the *P2<sub>1</sub>/n* space group and has *Z* = 4 molecules per unit cell;  $\beta$ -HNIW has *Pb2<sub>1</sub>a* symmetry, with *Z* = 4 molecules per unit cell; and the  $\gamma$ -phase has *P2<sub>1</sub>/n* symmetry, with *Z* = 4 molecules per unit cell. Figure 1 illustrates these polymorphs of HNIW; the  $\zeta$ -polymorph is evident at high pressure, but its crystal structure has not yet been resolved.<sup>4</sup> As evident in the figure, the molecular structure of the polymorphs differ mainly in the orientation of the nitro groups relative to the ring. Two different rankings of the relative stabilities of these polymorphs have been proposed:  $\alpha$ -hydrate >  $\epsilon$  >  $\alpha$ -anhydrous >  $\beta$  >  $\gamma$ <sup>6</sup> and  $\epsilon$  >  $\gamma$  >  $\alpha$ -hydrate >  $\beta$ .<sup>7</sup>

## Intermolecular Interaction Potential

For this study, we use the same values of the 6-exp potential parameters as in the RDX study.<sup>1</sup> The Coulombic terms are determined by fitting partial charges centered on each atom of the HNIW molecule to a quantum mechanically derived electrostatic potential, performed at the HF/6-31G\*\* level as described in the earlier study.<sup>1</sup> For the treatment of different phases of the HNIW crystal, we also assume that there exists a transferability of the electrostatic charges. Consequently, we have used in all calculations a single set of atom-centered charges determined for an HNIW molecule with atomic ar-

<sup>†</sup> Oklahoma State University.

<sup>‡</sup> Current mailing address: Department of Chemistry, University of Pittsburgh, Pittsburgh, PA 15260.

<sup>§</sup> The U.S. Army Research Laboratory.

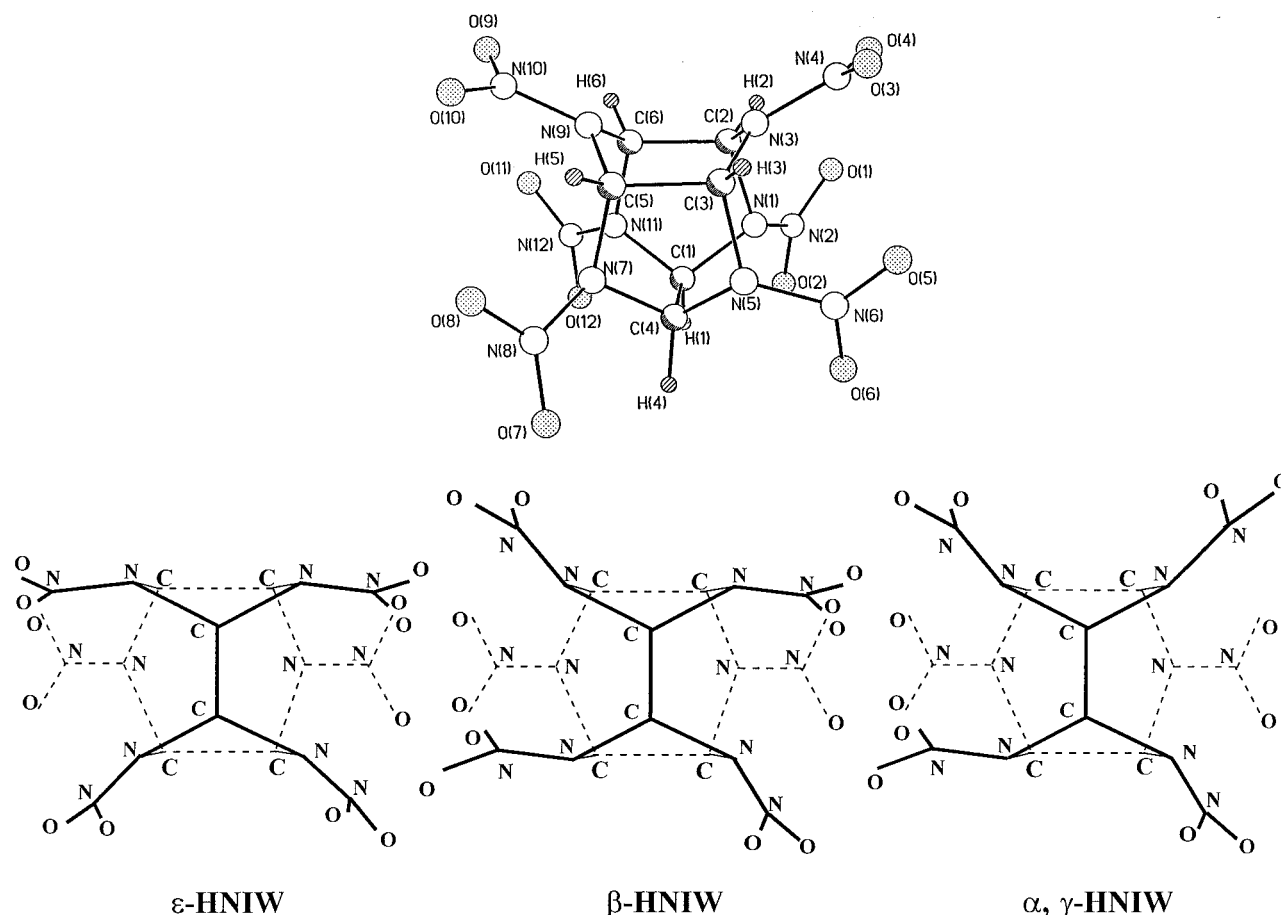


**Figure 1.** Molecular configuration of HNIW. Atom labels are consistent with the indices given in Table 1. Structures in the lower portion of the figure illustrate the differences between the polymorphic phases; the hydrogen atoms are not shown for clarity.

**TABLE 1: Electrostatic Charges for the HNIW Molecule**

atom <sup>a</sup>	charge/ $ e $	atom <sup>a</sup>	charge/ $ e $
C1	0.256 850	O1	-0.362 942
C2	0.183 418	O2	-0.369 093
C3	0.020 184	O3	-0.395 097
C4	0.089 133	O4	-0.377 983
C5	0.548 294	O5	-0.357 808
C6	0.368 468	O6	-0.431 362
N1	-0.196 698	O7	-0.395 640
N2	0.680 596	O8	-0.372 372
N3	-0.357 766	O9	-0.401 700
N4	0.786 509	O10	-0.416 611
N5	-0.326 781	O11	-0.381 535
N6	0.754 647	O12	-0.425 342
N7	-0.391 804	H1	0.112 444
N8	0.753 909	H2	0.117 717
N9	-0.577 874	H3	0.182 501
N10	0.844 354	H4	0.201 482
N11	-0.234 524	H5	0.081 152
N12	0.696 675	H6	0.094 597

<sup>a</sup> The atom indices are consistent with the labels in Figure 1.

rangement consistent with the crystallographic configuration of the  $\alpha$ -polymorph.<sup>4,8</sup> The resulting electrostatic charges are given in Table 1, and the parameters for the 6-exp terms are given in ref 1.

### Details of the Calculations

The tests of this potential were done by MP calculations with and without symmetry constraints and NPT-MD simulations at zero pressure over the temperature range 4.2–425 K for the  $\epsilon$ -,  $\beta$ -, and  $\gamma$ -polymorphs of HNIW. We do not report results of

$\alpha$ -HNIW, since no X-ray diffraction data are available for the anhydrous form of this polymorph. Also, the X-ray diffraction data for  $\alpha$ -hydrate HNIW is incomplete.<sup>5</sup> Thus, a suitable comparison between theoretical predictions and experiment for  $\alpha$ -HNIW is not possible at this time. In all calculations reported in this study, the crystal is represented as an ensemble of rigid molecules. The independent degrees of freedom are the six unit cell constants ( $a$ ,  $b$ ,  $c$ ,  $\alpha$ ,  $\beta$ ,  $\gamma$ ), the three rotations ( $\theta_1$ ,  $\theta_2$ ,  $\theta_3$ ), and the three translations ( $\tau_1$ ,  $\tau_2$ ,  $\tau_3$ ) for every molecule considered in the simulation. Details of the MP and NPT-MD calculations are described in ref 1 and briefly summarized below.

**a. Molecular Packing Calculations.** Two series of molecular packing calculations (minimizations of the lattice energy with respect to the structural degrees of freedom of the crystal) were performed. In the first series, using the program PCK91,<sup>9</sup> the space-group symmetries of the crystals were maintained throughout the energy minimization. In these calculations, all three dimensions of the unit cell and the three rotations and translations of the molecule in the asymmetric unit were allowed to vary, except for the case of the  $\beta$ -phase, where the translation along the  $b$ -axis was frozen due to the symmetry restrictions. The cell angles  $\alpha$ ,  $\beta$ , and  $\gamma$  were frozen at 90° for the calculations of the  $\beta$ -polymorph. For the  $\epsilon$ - and  $\gamma$ -polymorphs, the angle  $\beta$  of the unit cell was allowed to vary, and  $\alpha$  and  $\gamma$  were frozen at 90°. The positions and orientations of all other molecules in the unit cell are determined through symmetry operations relative to the molecule in the asymmetric unit.

A second series of MP calculations were performed in which the crystal symmetries are not constrained; the methods are described in our previous paper,<sup>1</sup> and the algorithm used is that

**TABLE 2: Lattice Parameters for Polymorphs of HNIW<sup>a</sup>**

lattice parameter	experiment <sup>4</sup>	PCK91	LMIN	NPT-MD <sup>b</sup>	
				4.2 K	300 K
$\epsilon$ -HNIW					
$a$ (Å)	8.8278	8.7973 (−0.4)	8.7948 (−0.4)	8.7953 (−0.4)	8.8420 (0.2)
$b$ (Å)	12.5166	12.4986 (−0.1)	12.4999 (−0.1)	12.5006 (−0.1)	12.5837 (0.5)
$c$ (Å)	13.3499	13.4071 (−0.4)	13.4055 (0.4)	13.4066 (0.4)	13.4897 (1.0)
$\alpha$ (deg)	90.000	90.000 <sup>c</sup>	89.998 (0.0)	90.000 (0.0)	89.999 (0.0)
$\beta$ (deg)	106.752	105.150 (−1.5)	105.137 (−1.5)	105.134 (−1.5)	105.377 (−1.3)
$\gamma$ (deg)	90.000	90.000 <sup>c</sup>	90.001 (0.0)	90.000 (0.0)	90.012 (0.0)
$\beta$ -HNIW					
$a$ (Å)	9.6764	9.5242 (−1.6)	9.5239 (−1.6)	9.5272 (−1.5)	9.6106 (−0.7)
$b$ (Å)	13.0063	12.8726 (−1.0)	12.8728 (−1.0)	12.7485 (2.0)	12.9316 (−0.6)
$c$ (Å)	11.6493	11.7025 (0.5)	11.7020 (0.4)	11.7050 (0.5)	11.7566 (0.9)
$\alpha$ (deg)	90.000	90.000 <sup>c</sup>	90.000 (0.0)	89.999 (0.0)	90.009 (0.0)
$\beta$ (deg)	90.000	90.000 <sup>c</sup>	89.999 (0.0)	90.000 (0.0)	90.009 (0.0)
$\gamma$ (deg)	90.000	90.000 <sup>c</sup>	90.000 (0.0)	90.000 (0.0)	89.999 (0.0)
$\gamma$ -HNIW					
$a$ (Å)	13.2310	13.4342 (1.5)	13.4348 (1.5)	13.4370 (−1.6)	13.5144 (2.1)
$b$ (Å)	8.1700	7.9095 (−3.2)	7.9074 (−3.2)	7.9092 (−3.2)	7.9690 (−2.5)
$c$ (Å)	14.8760	14.8531 (−0.2)	14.8519 (−0.2)	14.8548 (−0.1)	14.9413 (0.4)
$\alpha$ (deg)	90.000	90.000 <sup>c</sup>	90.000 (0.0)	90.000 (0.0)	89.986 (0.0)
$\beta$ (deg)	109.170	108.84 (0.3)	108.734 (−0.4)	108.863 (−0.3)	109.064 (−0.1)
$\gamma$ (deg)	90.000	90.000 <sup>c</sup>	90.001(0.0)	90.000 (0.0)	90.013 (0.0)

<sup>a</sup> Percent deviations from experiment in parentheses. <sup>b</sup> Time-averaged values (see text). <sup>c</sup> Fixed throughout calculation.

in the program LMIN.<sup>10</sup> In these calculations, the cutoff parameters *P* and *Q* (see ref 1 for their description) were set equal to 17.5 and 18.0, respectively.

**b. Isothermal–Isobaric Molecular Dynamics Calculations.** Simulations of the  $\epsilon$ -,  $\beta$ -, and  $\gamma$ -phases of the HNIW crystal at various temperatures in the range 4.2–425 K and at zero pressure were performed using the algorithm proposed by Nosé and Klein<sup>11</sup> as implemented in the program MDCSPC.<sup>12</sup> Details of the calculations are given in ref 1 and remain the same, with the following exceptions: The MD simulation cell consists of a box containing 12 ( $3 \times 2 \times 2$ ), 27 ( $3 \times 3 \times 3$ ), and 12 ( $2 \times 3 \times 2$ ) crystallographic unit cells for phases  $\epsilon$ ,  $\beta$ , and  $\gamma$ , respectively. The lattice sums were calculated in all dimensions in these simulations. The interactions were determined between the sites in the simulation box and the nearest-image sites within the cutoff distance. The cutoff distances are  $R_{\text{cut}} = 10.01$ , 11.61, and 9.80 Å for phases  $\epsilon$ ,  $\beta$ , and  $\gamma$ , respectively. For simulations at 4.2 K, the initial positions of the atoms are identical with those in the experimental structures. The equations of motion were integrated for 2000 time steps (1 time step =  $2 \times 10^{-15}$  s) to equilibrate the system. After the equilibration, an additional 5000 (for temperatures below 300 K) or 8000 (for temperatures between 300 and 425 K) steps were integrated, during which average properties were calculated. In subsequent runs for successively higher temperatures, the initial atomic positions and velocities are identical with those obtained at the end of the preceding lower-temperature simulation. The velocities were scaled over an equilibration period of 2000 steps, in order to achieve the desired external temperature and pressure, followed by the 5000- or 8000-step integration for calculation of averages. The cumulative mass-center radial distribution functions (RDF) and averages are calculated for the mass centers and Euler angles of the molecules. The RDFs and averages were obtained from values calculated at every 10th step during the trajectory integrations.

## Results and Discussions

**a. Molecular Packing Calculations.** The results of the MP calculations with (denoted as PCK91) and without (denoted LMIN) symmetry constraints are given in Table 2. The

relaxation of the symmetry conditions has a very small effect on the final geometric parameters, and both sets of MP calculations predict almost identical structures. Deviations of the cell lengths from experiment are less than 0.4%, 1.6%, and 3.2% for the  $\epsilon$ -,  $\beta$ -, and  $\gamma$ -phases, respectively. For those crystal symmetries in which the  $\beta$  cell angle was allowed to vary during minimization (the  $\epsilon$ - and  $\gamma$ -phases), deviations of this angle from experiment are no greater than 1.5%. Lattice energies per molecule for the  $\epsilon$ -,  $\beta$ -, and  $\gamma$ -HNIW phases (−210.47, −207.43, and −201.42 kJ/mol, respectively) support the polymorph stability ranking of  $\epsilon > \beta > \gamma$  given by Russell et al.<sup>6</sup> Small differences in the total lattice energies (<0.5 kJ/mol) between the constrained and unconstrained calculations are due to the fact that the unconstrained simulations do not use the accelerated convergence method for evaluation of the  $1/r^6$  lattice sums.

**b. NPT Molecular Dynamics Calculations.** The analysis of time histories (not shown) of the lattice parameters (*a*, *b*, *c*,  $\alpha$ ,  $\beta$ ,  $\gamma$ ) indicate that these properties are well behaved after the equilibrium is reached; i.e., each parameter oscillates about the average value for the duration of the trajectory. Time histories of the rotational and translational temperatures and for the pressure show similar behavior, indicating that the system is at thermodynamic equilibrium.

The crystal structure information resulting from NPT-MD simulations at zero pressure, *T* = 4.2 and 300 K, is given in Table 2. The lattice dimensions obtained at *T* = 4.2 K are in very close agreement with those determined in the MP calculations. This is expected, since the thermal effects at 4.2 K should be minimal and the thermal averages at this temperature should be close to the values corresponding to the potential energy minimum. At 300 K, the average lattice dimensions agree very well with the experimental values, the corresponding differences for *a*, *b*, and *c* cell lengths being, respectively, 0.2%, 0.5%, and 1.0% for the  $\epsilon$ -phase, 0.7%, 0.6%, and 0.9% for the  $\beta$ -phase, and 2.1%, 2.5%, and 0.4% for the  $\gamma$ -phase. For the  $\epsilon$ - and  $\gamma$ -phases, the variations of the unit cell angle  $\beta$  from the experimental values are 1.3% and 0.1%, respectively, while the other two angles of the unit cell remain approximately equal to 90°. For the  $\beta$ -phase, all three crystallographic angles remain approximately equal to 90°, in agreement with experiment.

**TABLE 3: Parameters for Linear Fits in Temperature<sup>a</sup> and Thermal Expansion Coefficients ( $T = 300$  K) of Unit Cell Edge Lengths and Volumes**

	$\epsilon$ -HNIW			$\beta$ -HNIW			$\gamma$ -HNIW		
	$\chi_0^b$	$\chi_1^c$	expansion coef. ( $K^{-1}$ ) <sup>c</sup>	$\chi_0^b$	$\chi_1^c$	expansion coef. ( $K^{-1}$ ) <sup>c</sup>	$\chi_0^b$	$\chi_1^c$	expansion coef. ( $K^{-1}$ ) <sup>c</sup>
<i>a</i>	8.7939	$1.5537 \times 10^{-4}$	$1.76 \times 10^{-5}$	9.5234	$2.8119 \times 10^{-4}$	$2.93 \times 10^{-5}$	13.4285	$2.8185 \times 10^{-4}$	$2.09 \times 10^{-5}$
<i>b</i>	12.4982	$2.8271 \times 10^{-4}$	$2.25 \times 10^{-5}$	12.8702	$2.1988 \times 10^{-4}$	$1.70 \times 10^{-5}$	7.9091	$1.9651 \times 10^{-4}$	$2.47 \times 10^{-5}$
<i>c</i>	13.4050	$2.8676 \times 10^{-4}$	$2.13 \times 10^{-5}$	11.7011	$1.9738 \times 10^{-4}$	$1.68 \times 10^{-5}$	14.8493	$3.0343 \times 10^{-4}$	$2.03 \times 10^{-5}$
<i>V</i>	1422.253	$8.2276 \times 10^{-2}$	$5.69 \times 10^{-5}$	1434.150	$9.1771 \times 10^{-2}$	$6.28 \times 10^{-5}$	1492.486	$9.3136 \times 10^{-2}$	$6.13 \times 10^{-5}$

<sup>a</sup>  $X = \chi_0 + \chi_1 T$ ,  $X = a, b, c$ , or  $V$ . <sup>b</sup> Units of Å for  $a, b$ , and  $c$ ; units of Å<sup>3</sup> for volume  $V$ . <sup>c</sup> Units of Å/K for  $a, b$ , and  $c$ ; units of Å<sup>3</sup>/K for volume  $V$ .

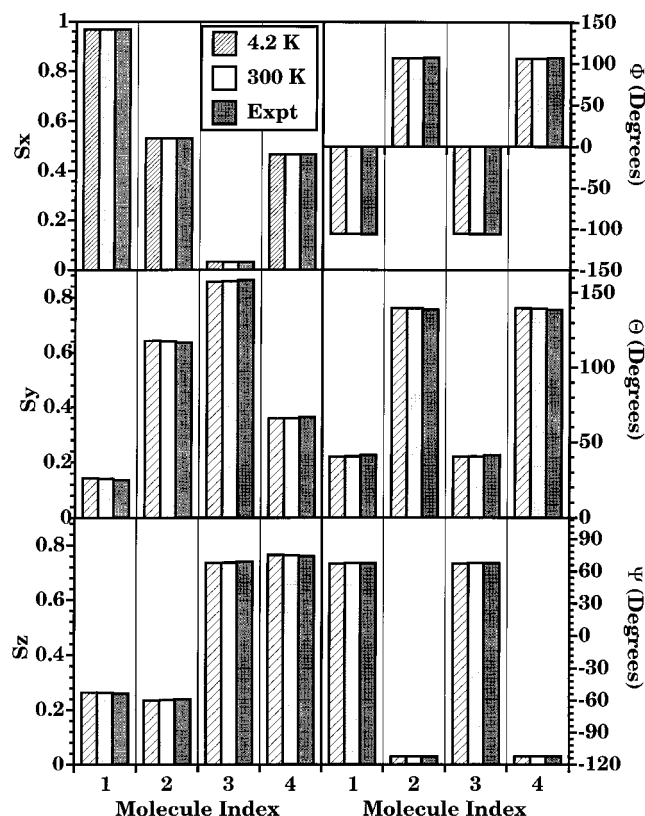


**Figure 2.** Comparison of the time-averaged mass-center fractional positions and Euler angles (X-convention<sup>13</sup>) with experimental results at 300 K and 0 atm for the  $\epsilon$ -phase. These time averages for each molecule in the unit cell are over all unit cells in the simulation box.

Figure 2 provides a visual comparison of the average mass-center fractionals and Euler angles for each of the four molecules within the unit cell of  $\epsilon$ -HNIW with experimental values; the data for the three polymorphs of HNIW are given in Supporting Information Table 1S. Increasing the temperature from 4.2 to 300 K does not produce any significant displacement of the molecular mass-centers or increase the degree of rotational disorder. In addition, there is a slightly better agreement with experiment for the orientational parameters and fractional coordinates of the molecules at 300 K than at lower temperatures.

Similar good agreement with experiment exists for predictions of  $\beta$ - and  $\gamma$ -HNIW (not shown). The largest deviation between experiment and predictions of molecular orientation occurs for the Euler angle  $\Phi$  for  $\gamma$ -HNIW; the predicted value is 4.4° larger than the experimental value.

The mass-center—mass-center RDFs for the  $\epsilon$ -polymorph (Figure 3) exhibit well-ordered structures with correlation at long distances at higher temperatures. The positions of the major peaks do not change significantly, and the main temper-

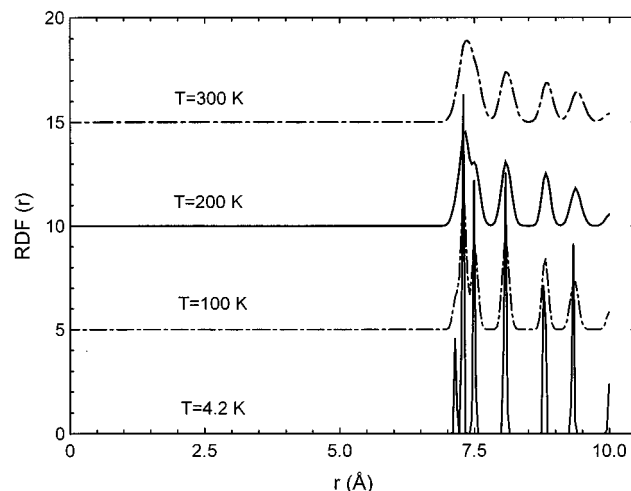


**Figure 3.** Radial distribution function (RDF) for mass-center—mass-center pairs as functions of temperature for the  $\epsilon$ -phase.

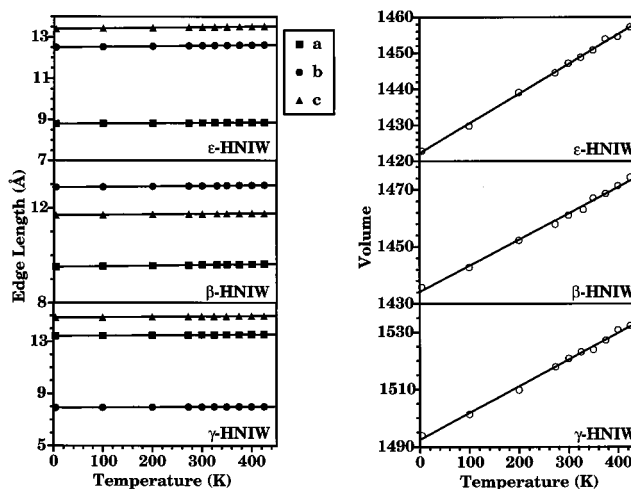


**Figure 4.** Unit cell edge lengths and volumes as functions of temperature for  $\epsilon$ -HNIW (upper frames),  $\beta$ -HNIW (middle frames), and  $\gamma$ -HNIW (lower frames). The symbols denote time averages, and the solid curves are linear fits of the points (coefficients given in Table 3).

ature effect is the broadening of the peaks and partial overlapping of some of them. The features of the RDFs for the  $\beta$ - and  $\gamma$ -phases are similar to those shown in Figure 3.

Finally, the cell edge lengths and volumes have a linear dependence on temperature over the range 4.2–425 K, as evident in Figure 4. Linear and volume thermal expansion coefficients are determined from linear least-squares fits to these data, the parameters of which are listed in Table 3. The linear and volume expansion coefficients

$$C_X = \frac{1}{X} \left( \frac{\partial X}{\partial T} \right) \quad (1)$$

where  $X$  denotes cell edge lengths  $a$ ,  $b$ , or  $c$  or volume  $V$  and  $C_X$  is the corresponding thermal expansion coefficient, were calculated at  $T = 300$  K; they are given in Table 3 for the three polymorphic phases. The results indicate a near isotropic thermal expansion for the  $\epsilon$ - and  $\gamma$ -phases (coefficients are within  $\sim 20\%$  of one another) and anisotropic expansion for  $\beta$ -HNIW. For  $\beta$ -HNIW, the linear expansion coefficient for cell edge  $a$  is  $\sim 70\%$  larger than those for  $b$  and  $c$ . The volume expansion coefficients for the three polymorphs have similar values ( $\sim 6 \times 10^{-5} \text{ K}^{-1}$ ). At present, no experimental data are available to which the calculated thermal coefficients can be compared, and it is hoped that these results will stimulate measurement of these properties.

## Conclusion

We have performed molecular packing and NPT-MD simulations of three phases ( $\epsilon$ ,  $\beta$ , and  $\gamma$ ) of the 2,4,6,8,10,12-hexanitrohexaazaisowurtzitane (HNIW) crystal using 6-exp Buckingham potentials developed for the RDX crystal,<sup>1</sup> plus Coulombic interactions using electrostatic charges determined from fits to ab initio electrostatic potentials calculated at the HF/6-31G\*\* level. Molecular packing calculations with and without symmetry constraints show good agreement between predicted geometrical parameters and experimental values for all three phases. Additionally, the calculations indicate a stability ranking order  $\epsilon > \beta > \gamma$  in agreement with experimental measurement.<sup>6</sup> NPT-MD predictions of crystal parameters at room temperature and zero pressure agree with the experimental unit cell dimensions to within 1.0% for phase  $\epsilon$ , 0.9% for phase  $\beta$ , and 2.5% for phase  $\gamma$ . Additionally, little rotational or translational disorder occurs in thermal, unconstrained trajectories.

Temperature dependencies of the physical parameters of the lattice at zero pressure over the temperature range 4.2–425 K indicate that thermal expansion of the three crystalline polymorphs is nearly isotropic for  $\epsilon$ - and  $\gamma$ -HNIW and is anisotropic for  $\beta$ -HNIW.

The success of the present potential energy parameters in describing different phases of the HNIW crystal at moderate temperatures and low pressure provides incentive to further investigate the transferability of this model to other cyclic nitramine systems (e.g., HMX) and more dissimilar energetic crystals (TNT, TATB). Future work will be directed to determining the degree to which this potential energy function is transferable to other energetic materials. Incorporation of intramolecular motion by relaxing the rigid molecular model will also be investigated.

**Acknowledgment.** This work was supported by the Strategic Environmental Research and Development Program. The authors

thank Dr. Richard Gilardi, Naval Research Laboratory, for kindly providing the X-ray diffraction data for HNIW. D.L.T. gratefully acknowledges support by the U.S. Army Research Office under grant number DAAH04-93-G-0450.

**Supporting Information Available:** Tables giving fractional coordinates and Euler angles of the molecular mass-center and NPT-MD lattice dimensions for  $\epsilon$ -,  $\beta$ -, and  $\gamma$ -HNIW (3 pages). Ordering information is given on any current masthead page.

## References and Notes

- (1) Sorescu, D. C.; Rice, B. M.; Thompson, D. L. *J. Phys. Chem. B* **1997**, *101*, 798.
- (2) Miller, R. S. In *Decomposition, Combustion and Detonation Chemistry of Energetic Materials*; Brill, T. B., Russell, T. P., Tao, W. C., Wardle, R. B., Eds.; Materials Research Society Symposium Proceedings 418; Materials Research Society: Pittsburgh, PA, 1995; p 3.
- (3) For a compilation of information about HNIW, see: Filliben, Jeff D., Ed. *CPIA/M3 Solid Propellant Ingredients Manual*; Publication Unit 89; Chemical Propulsion Information Agency, 10630 Little Patuxent Parkway, Suite 202, Columbia, MD, 21044-3200. Distribution authorized to U.S. Government agencies only; test and evaluation; Sep 1994. Other requests for this document shall be referred to the Office of Naval Research, Code ONR-35, Arlington, VA 22217-5000.
- (4) Chan, M. L.; Carpenter, P.; Hollins, R.; Nadler, M.; Nielsen, A. T.; Nissan, R.; Vanderah, D. J.; Yee, R.; Gilardi, R. D. CPIA-PUB-625, Apr 95, 17P, CPIA Abstract No. X95-07119, AD D606 761. Availability: Distribution authorized to the Department of Defense and DoD contractors only; Critical Technology; March 17, 1995. Other requests shall be referred to the Naval Air Warfare Center Weapons Division (474000D), China Lake, CA 93555-6001. This document contains export-controlled technical data.
- (5) The X-ray diffraction data corresponds to the hydrated crystal, in which the number and orientation of the water molecules are not resolved (R. D. Gilardi, private communication).
- (6) Russell, T. P.; Miller, P. J.; Piermarini, G. J.; Block, S.; Gilardi, R.; George, C. AD-C048 931 (92-0134), p 155, Apr 91, CPIA Abstract No. 92, 0149, AD D604 542, C-D, Chemical Propulsion Information Agency, 10630 Little Patuxent Parkway, Suite 202, Columbia, MD 21044-3200.
- (7) Foltz, M. F.; Coon, C. L.; Garcia, F.; Nichols, A. L., III. AD-C049 633L (93-0001), p 9, Apr 92, Contract W-7405-ENG-48, CPIA Abstract No. 93-0003, AD D605 199, U-D, Chemical Propulsion Information Agency, 10630 Little Patuxent Parkway, Suite 202, Columbia, MD 21044-3200.
- (8) MP (PCK91) calculations using HF/6-31G\*\* atomic charges determined for HNIW with molecular arrangements consistent with the  $\beta$ - and  $\gamma$ -polymorphic crystallographic configurations predict lattice parameters similar to those that use HF/6-31G\*\* atomic charges assuming the  $\alpha$ -hydrate HNIW molecular configuration. Cell edge lengths differ by no more than 0.015 Å, and cell angles differ by less than 0.17°. The electrostatic energies differ by less than 5 kJ/mol.
- (9) Williams, D. E. PCK91, a Crystal Molecular Packing Analysis Program, Department of Chemistry, University of Louisville, Louisville, KY 40292.
- (10) Gibson, K. D.; Scheraga, H. A. LMIN: A Program for Crystal Packing, QCPE No. 664.
- (11) Nosé, S.; Klein, M. L. *Mol. Phys.* **1983**, *50*, 1055.
- (12) Smith, W. MDCSPC, Version 4.3, A Program for Molecular Dynamics Simulations of Phase Changes, CCP5 Program Library (SERC), May 1991.
- (13) Goldstein, H. *Classical Mechanics*; Addison-Wesley: Reading, MA, 1980.